JOURNAL OF MATERIALS SCIENCE 13 (1978) 2394–2402

Structural studies of compounds in the series $GaS_xSe_{(1-x)}$ ($0 \leqslant x \leqslant 1$) grown by iodine vapour transport

C.R. WHITEHOUSE,* A.A. BALCHIN
Crystallography Laboratory, Department of Applied Physics, Brighton Polytechnic, Moulsecoomb, Brighton, UK

A discontinuity in the length of the c-axis of compounds in the series $GaS_xSe_{(1-x)}$ is observed at the composition $x = 0.25$. This is thought to be caused by a transition from the β structure of GaS to the ϵ structure of GaSe. Although lattice parameter measurements indicate that the transition is abrupt, structure factor calculations and observations of the form of the (0 0 0 1) surface growth features indicate that the transition is not sharp, but takes place over the composition range $0.2 \leqslant x \leqslant 0.3$. Growth features change in form as x varies, from hexagonal spirals characteristic of GaS to triangular spirals typical of GaSe.

1. Introduction

Both gallium selenide and gallium sulphide crystals consist of four-fold atomic layers of the type Se(or S)–Ga–Ga–Se(or S), but differ in the way the layers are stacked. Gallium selenide may exist in any one of four different crystalline forms. The β and ϵ forms are 2H with stacking $A\beta\beta A$ $B\alpha\alpha B$ and $A\beta\beta A$ $B\gamma\gamma B$ respectively. γ is 3R with stacking $A\beta\beta A$ $B\gamma\gamma B$ $C\alpha\alpha C$ [1–3], while the δ-form is 4H with stacking $A\beta\beta A$ $C\alpha\alpha C$ $A\gamma\gamma A$ $B\alpha\alpha B$ [4]. In β-GaSe, which is isomorphous with GaS, each layer can be converted to its neighbour by a translation in a $\langle 1\,0\,\bar{1}\,0\rangle$ direction followed by a rotation of $60°$ about the [0 0 0 1] c-axis. In the ϵ- and γ-GaSe structures each layer can be converted to its neighbour by only a translation in the $\langle 1\,0\,\bar{1}\,0\rangle$ direction. The structures are shown in Fig. 1.

Terhell and Lieth [5] have shown that powdering destroys the low degree of order of the ϵ-form of GaSe, and they question the existence of a distinctive β-phase. However, from their observations of the presence of a sharp discontinuity in the unit-cell c-parameter for the $GaS_xSe_{(1-x)}$ series, and also from the similarity of line broadening effects on X-ray photographs of compounds for which $x \leqslant 0.25$, they suggest that all mixed compounds of $x \geqslant 0.25$ possess the β-structure. Structure factor calculations in support of their suggestion have not been presented. Manfredotti *et al.* [6] conclude from optical absorption measurements that the β-structure is dominant over the whole range of $GaS_xSe_{(1-x)}$ compounds grown by iodine vapour transport, but point out that electron diffraction measurements [7] also confirm the c-axis discontinuity near $x = 0.25$.

Since the selenium and the sulphur atoms may occupy equivalent sites in the four-fold layer, it is well known [8–11] that it is possible to obtain a continuous range of solid solutions in the series $GaS_xSe_{(1-x)}$ ($0 \leqslant x \leqslant 1$). Although several authors [8, 10, 12] have reported the growth of these compounds by the iodine vapour transport technique, only Terhell and Lieth [8] and Manfredotti *et al.* [6] give full information regarding growth conditions used; some crystal growth data is, however, also included by Arancia, Grandolfo, Manfredotti and Rizzo [7].

2. Experimental results

2.1. Crystal growth

As part of a more extensive research programme, additional compounds of the series $GaS_xSe_{(1-x)}$

*Now at: The Merz Laboratory, Department of Electrical and Electronic Engineering, The University of Newcastle-upon-Tyne, UK.

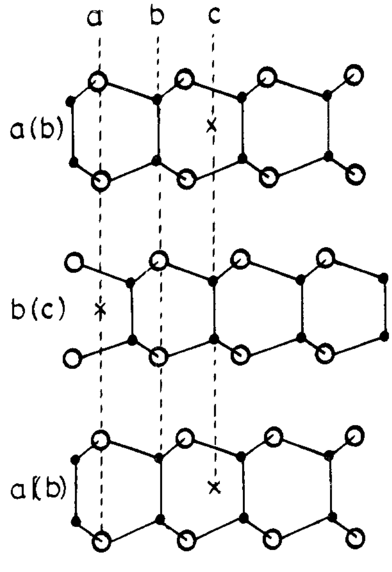

(a) ϵ - GaSe (hexagonal)

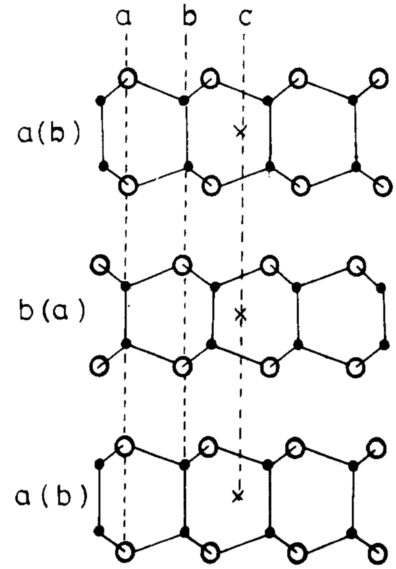

(c) GaS, β - GaSe (hexagonal)

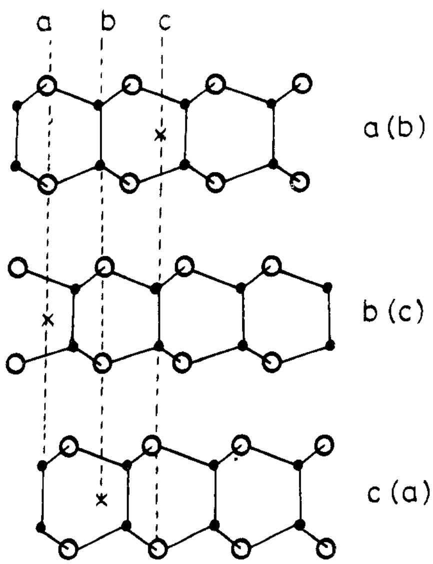

(b) γ - GaSe (rhombohedral)

Figure 1 The ϵ, γ and β forms of GaSe, and β-GaS.

have been grown in the region of the previously reported [7, 8] c-axis discontinuity in an attempt to gain further information concerning structural transformations near $x = 0.25$. Where possible structures have been identified from a comparison of observed and calculated structure factors.

Using iodine vapour transport driven by a temperature gradient in evacuated growth ampoules, a comprehensive series of experiments [13] fixed the optimum reaction and growth conditions for gallium selenide single crystals at 850° C and 750° C respectively. A similar determination of optimum growth conditions for gallium sulphide fixed these reaction and growth temperatures at 910° C and 850° C. For the growth of the series $GaS_xSe_{(1-x)}$ a linear interpolation of the reaction and growth temperatures with the composition variable, x, between these two sets of extreme values yielded growth of a well-separated selection of large single crystals, distributed with little intergrowth over the whole of the cooler region of the ampoule. The actual values of the temperatures used were not critical, but temperature stability (± 1° C) was most important.

The growth ampoules used were 200 mm long × 15.70 mm internal diameter. Stoichiometric weights of high purity elements gallium, selenium and sulphur were used, corresponding to a total charge of 1.90 g in each growth experiment. An initial iodine concentration between 2.0 and 4.0 mg per cm^3 of ampoule volume was used. Growth times varied from 20 to 200 h depending on the sizes of the single crystals required. Crystals 10 mm × 10 mm in superficial area and of thickness varying from 0.07 mm ($x < 0.25$) to 0.01 mm ($x > 0.25$) formed in a growth period of 150 h. The growth parameters used in this work are comparable with those of Terhell and Lieth [8]. The single crystals grown varied in colour as chemical composition changed, from the pale yellow of pure GaS via orange to the dark red of pure GaSe.

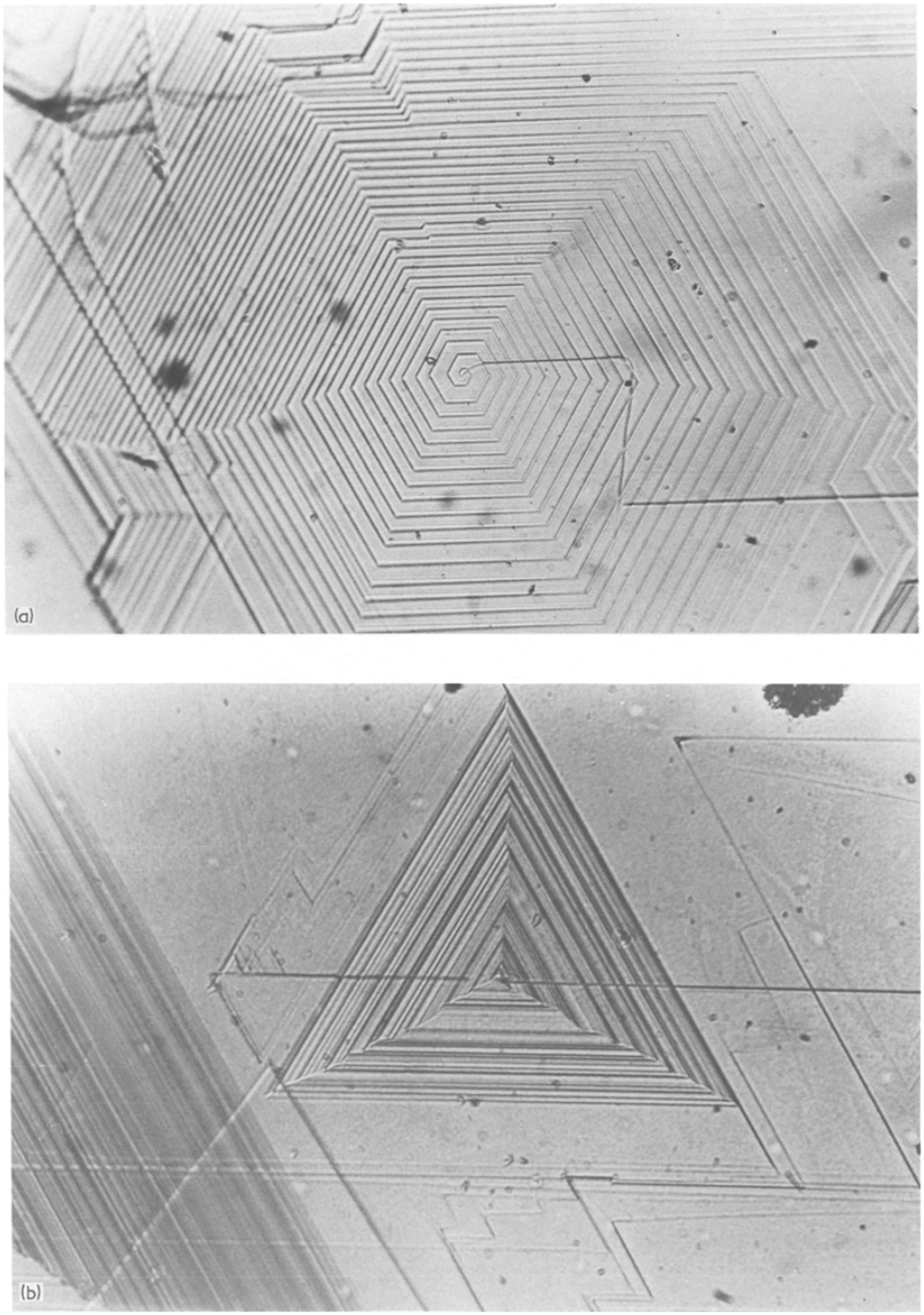

Figure 2 (a) A hexagonal growth spiral typical of those found on single crystals of gallium sulphide. (b) Triangular growth spirals typical of those formed on gallium selenide.

2.2. Surface growth features

All the single crystals grown in the series exhibited characteristic growth spirals, suggesting that a screw dislocation mechanism plays an important part [14–16] in the growth of these compounds by iodine vapour transport. Earlier studies by Bolsterli and Mooser [11] have shown that the structural differences between GaS and GaSe result in a variation in the geometry of the growth features formed on the single crystal $GaS_xSe_{(1-x)}$ solid solutions. In agreement with this work it was observed that GaS grown in the present investigation showed regular hexagonal growth spirals on (0 0 0 1), with equal step widths between the spiral arms (a typical example is shown in Fig. 2a). In contrast, the GaSe single crystals usually, but not always, showed growth spirals in the form of perfect equilateral triangles (Fig. 2b). In several cases these triangular growth spirals were truncated at the apices, and sometimes – although rarely – totally non-polygonized growth spirals were observed, similar to those described by Lendvay *et al.* [16].

Back reflection Laue X-ray photographs indicated that in the case of GaS the edges of the hexagonal spirals formed $\{1\,0\,\bar{1}\,0\}$ planes. Such planes are symmetrical in both gallium and sulphur atoms and hence it is to be expected that growth on each of the six fronts would be equally favoured. In GaSe it was found that the three edges of the triangular growth features formed three of the six $\{1\,0\,\bar{1}\,0\}$ planes, such as $(1\,0\,\bar{1}\,0)$, $(0\,\bar{1}\,1\,0)$, $(1\,\bar{1}\,0\,0)$. This is in agreement with the findings of Bolsterli and Mooser [11] but is in contrast to the conclusions of Kuhn *et al.* [15], who describe a differing orientation for the triangular growth spirals.

On a few, rare, occasions, simultaneous occurrence was observed on GaSe crystals of two different forms of the triangular growth features, by which one of the triangles was rotated through 60° about [0 0 0 1] with respect to the other. The growth fronts on this second type of spiral formed the three remaining $\{1\,0\,\bar{1}\,0\}$ planes, namely $(\bar{1}\,0\,1\,0)$, $(0\,1\,\bar{1}\,0)$, $(\bar{1}\,1\,0\,0)$. From a consideration of the ϵ and γ structures of GaSe (see Fig. 3) it is found that, except at the apices, the first type of triangular spiral is bounded by triply bonded gallium atoms, whereas the second type is bounded by doubly bonded selenium. It is therefore reasonable that growth in GaSe should proceed at different rates in opposing $\langle 1\,0\,\bar{1}\,0\rangle$ directions. In each case the slower growing $\{1\,0\,\bar{1}\,0\}$ faces would be over-ridden by the faster growing ones, and growth spirals in the form of equilateral triangles would result. The formation of truncated growth spirals is then attributable to supression of the growth of one of the rapidly growing $\{1\,0\,\bar{1}\,0\}$ faces, possibly by the presence of impurity atoms or crystal defects. The mechanism described is supported by studies of chemical etching [14, 16] and renders untenable the growth mechanism suggested by Kuhn *et al.* [15].

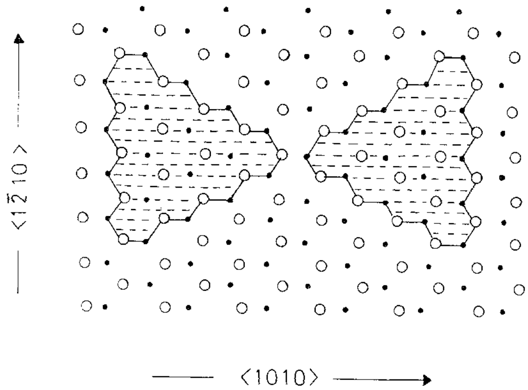

Figure 3 Two possible orientations of triangular growth spirals on the ϵ or γ forms of GaSe. The dark circles represent gallium and the open circles selenium.

Growth features observed on single crystals belonging to the series $GaS_xSe_{(1-x)}$ are found to vary in shape according to the value of the composition variable x. A transition from the triangular growth features characteristic of GaSe to the hexagons of GaS is observed as x varies from 0 to 1. Within the composition range $0.3 \leqslant x \leqslant 1$, all the crystals examined (about 200) showed hexagonal growth spirals. At lower values of x, $0 \leqslant x \leqslant 0.2$, the growth features were more complex, and consisted of intersecting hexagons and triangles. Only rarely were isolated hexagons seen at low values of x. Although the transition in the shapes of the growth spirals is not sharply defined, it is consistent with a change in structure as we pass through the series between GaS and GaSe.

2.3. X-ray studies of the series $GaS_xSe_{(1-x)}$

The crystal structure parameters of the hexagonal unit cells were measured from Debye–Scherrer powder X-ray photographs taken using CuKα radiation. They are plotted in Fig. 4. The variation of length of the hexagonal a-axis with composition, x, is linear and accords with Vegard's Law. Intro-

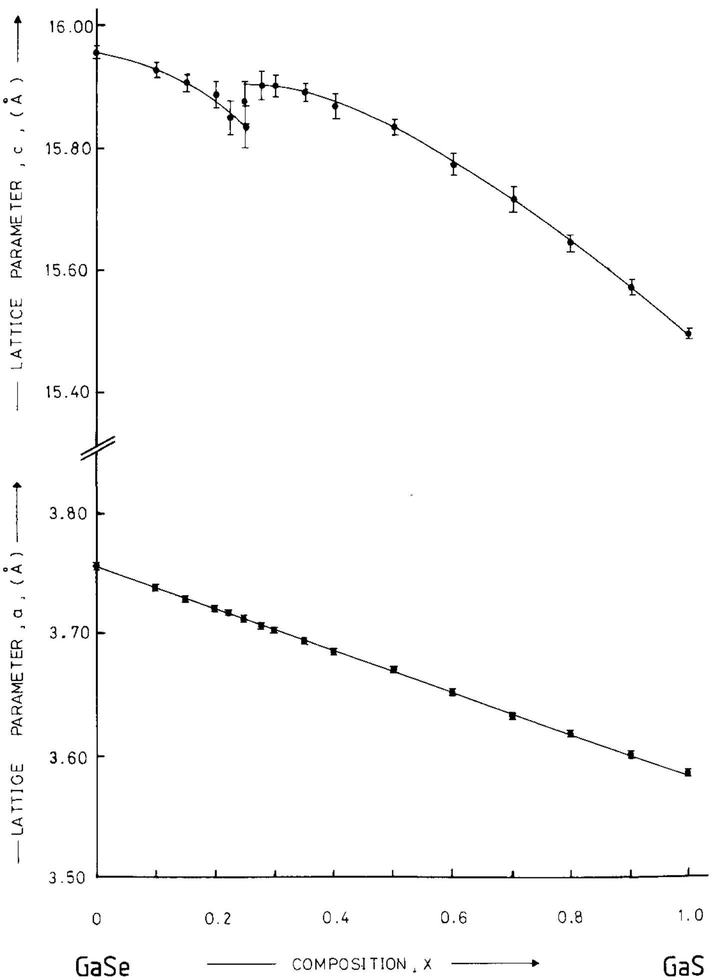

Figure 4 Variation of unit cell parameters, a and c, with composition variable x.

duction of increasing amounts of the larger selenium atoms into the lattice of gallium sulphide results in an increase in a according to the equation:

$$a(x) = 3.754 - 0.170x \text{ (Å)}$$

In contrast, variation of the c-axis is appreciably non-linear, with a sharp discontinuity at the composition $GaS_{0.25}Se_{0.75}$. For values of x in the range $0 \leqslant x \leqslant 0.25$, the c-axis variation is of the form:

$$c(x) = 15.960 - 0.111x - 1.402x^2 \text{ (Å)}$$

whilst for $0.25 \leqslant x \leqslant 1.0$,

$$c(x) = 15.990 - 0.150x - 0.339x^2 \text{ (Å)}$$

Good reproducibility of measured parameters is found, both when samples are taken from different regions of a single growth ampoule, and when different growth ampoules of the same nominal composition are sampled. Sample compositions were confirmed by an oxide reduction technique, by measuring the increase in weight when the samples were oxidized to Ga_2O_3. A comparison is made with previously reported values of lattice parameters for GaS and GaSe in Table I. For crystals of composition near the discontinuity, line broadening effects caused a considerable decrease in accuracy of the measurements of the c-parameter. Terhell and Lieth [8] observed discontinuities in both a and c in the region of $x = 0.25$, but their data is insufficient in this region to resolve clearly the variations of lattice parameter. The present measurements, except in the region of the discontinuity, are in good agreement with their values. Arancia *et al.* [7] give values for a and c for members of the series, measured by electron diffraction for both Bridgmann–Stockbarger and vapour-grown crystals. Their results are more in line with the present observations, in that no discontinuity is found in the values of the a-parameter, although a discontinuity is measured in

TABLE I Comparison of the crystal parameters of GaS and GaSe measured in the present work with those quoted by previous workers

Symmetry type	a(Å)	c (Å)	Reference
GaS			
β	3.578 kX	15.47 kX	[1]
β	3.575 kX (= 3.585 Å)	15.47 kX (= 15.50 Å)	[17]
β	3.586 ± 0.002	15.500 ± 0.003	[8]
–	3.596 ± 0.005	15.55 ± 0.02	[7] Bridgmann
–	3.593 ± 0.005	15.54 ± 0.02	[7] Vapour grown
β	3.586 ± 0.002	15.498 ± 0.008	Present study
GaSe			
β	3.752	15.95	[1]
ϵ	3.742	15.919	[18]
γ	3.746	23.910	[3]
β	3.755	15.44	[2]
γ	3.755	23.92	[2]
ϵ	3.755 ± 0.002	15.946 ± 0.003	[8]
–	3.759	16.02	[19]
–	3.749 ± 0.005	16.05 ± 0.02	[7] Bridgmann
–	3.738 ± 0.005	16.08 ± 0.02	[7] Vapour grown
δ	3.755	31.990	[4]
–	3.755 ± 0.002	15.955 ± 0.012	Present study

the c-axial length. Their measured parameters are in general greater than those of Terhell and Lieth. A detailed comparison between the present results and these earlier values is presented in Table II.

Powder X-ray photographs of compounds near the transition are shown in Fig. 5. Structure factor comparisons between the β and the ϵ structures for two of these compositions are made in Tables III and IV. For values of x in the range 0 to 0.25 line broadening similar to that observed on powder photographs of GaSe was found. This broadening was absent from the range $0.25 \leqslant x \leqslant 1$. For the compound $GaS_{0.25}Se_{0.75}$ line broadening varied from sample to sample. Compounds showing it are thought to have a structure identical to GaSe.

From a consideration of the intensity calculations, only a few of which are presented here, it is clear that for all values of x, comparisons of computed and observed intensities do not fit the γ-structure. The γ-structure is therefore not observed in any of the compounds grown. The powder patterns of GaS and of all the $GaS_xSe_{(1-x)}$

TABLE II Comparison of lattice parameters for solid solutions, $GaS_xSe_{(1-x)}$, with those measured by other workers

x	a (Å)	c (Å)	c/a
Present work			
0.00 (GaSe)	3.755 ± 0.002	15.959 ± 0.012	4.250
0.10	3.739 ± 0.003	15.930 ± 0.011	4.260
0.15	3.729 ± 0.002	15.912 ± 0.013	4.267
0.20	3.720 ± 0.003	15.892 ± 0.021	4.272
0.225	3.717 ± 0.004	15.849 ± 0.023	4.263
0.25	3.712 ± 0.004	15.833 ± 0.037	4.265
	3.710 ± 0.004	15.874 ± 0.039	4.279
0.275	3.706 ± 0.002	15.916 ± 0.012	4.295
0.30	3.701 ± 0.003	15.905 ± 0.020	4.297
0.35	3.694 ± 0.002	15.893 ± 0.010	4.302
0.40	3.686 ± 0.002	15.872 ± 0.018	4.306
0.50	3.670 ± 0.003	15.836 ± 0.013	4.315
0.60	3.653 ± 0.002	15.773 ± 0.014	4.318
0.70	3.632 ± 0.003	15.716 ± 0.022	4.327
0.80	3.618 ± 0.002	15.645 ± 0.013	4.324
0.90	3.600 ± 0.002	15.573 ± 0.010	4.325
1.00	3.586 ± 0.002	15.498 ± 0.008	4.321
Terhell and Lieth [8]			
0.0	3.755 ± 0.002	15.946 ± 0.003	4.25
0.1	3.736 ± 0.002	15.938 ± 0.003	4.27
0.2	3.719 ± 0.002	15.889 ± 0.003	4.27
0.25	3.689 ± 0.002	15.871 ± 0.003	4.30
0.3	3.700 ± 0.002	15.901 ± 0.003	4.30
0.4	3.684 ± 0.002	15.872 ± 0.003	4.31
0.5	3.672 ± 0.002	15.832 ± 0.003	4.31
0.6	3.655 ± 0.002	15.780 ± 0.003	4.32
0.7	3.632 ± 0.002	15.719 ± 0.003	4.33
0.8	3.621 ± 0.002	15.662 ± 0.003	4.33
0.9	3.600 ± 0.002	15.586 ± 0.003	4.33
1.0	3.586 ± 0.002	15.500 ± 0.003	4.32
Arancia *et al.* [7] Bridgmann – Stockbarger grown			
0.00	3.749 ± 0.005	16.05 ± 0.02	4.28
0.11	3.746 ± 0.005	16.02 ± 0.02	4.28
0.19	3.733 ± 0.005	15.95 ± 0.02	4.27
0.30	3.708 ± 0.005	15.87 ± 0.02	4.28
0.42	3.691 ± 0.005	15.78 ± 0.02	4.27
0.51	3.687 ± 0.005	15.96 ± 0.02	4.33
0.56	3.671 ± 0.005	15.88 ± 0.02	4.32
0.70	3.646 ± 0.005	15.75 ± 0.02	4.32
0.80	3.633 ± 0.005	15.69 ± 0.02	4.32
0.88	3.621 ± 0.005	15.66 ± 0.02	4.32
1.00	3.596 ± 0.005	15.55 ± 0.02	4.32
Arancia *et al.* [7] Vapour grown			
0.00	3.738 ± 0.005	16.08 ± 0.02	4.28
0.09	3.747 ± 0.005	16.03 ± 0.02	4.28
0.18	3.728 ± 0.005	15.97 ± 0.02	4.28
0.31	3.700 ± 0.005	16.04 ± 0.02	4.32
0.41	3.699 ± 0.005	16.01 ± 0.02	4.33
0.47	3.684 ± 0.005	15.92 ± 0.02	4.32
0.58	3.659 ± 0.005	15.81 ± 0.02	4.32
0.63	3.648 ± 0.005	15.78 ± 0.02	4.32
0.78	3.632 ± 0.005	15.69 ± 0.02	4.32
0.92	3.616 ± 0.005	15.63 ± 0.02	4.32
1.00	3.593 ± 0.005	15.54 ± 0.02	4.32

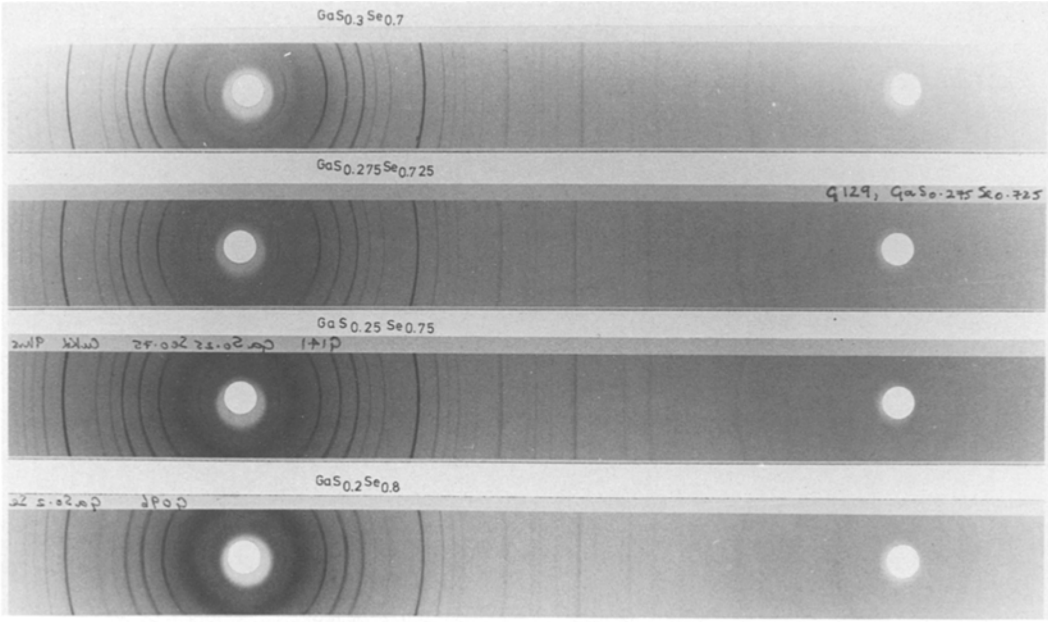

Figure 5 Powder photographs of $GaS_xSe_{(1-x)}$ for $x = 0.3$, 0.275, 0.25, 0.2 in the region of the structure transition.

TABLE III A comparison of the experimentally-observed and computed X-ray powder intensity data for the β- and ϵ-type structures of $GaS_{0.2}Se_{0.8}$ (CuKα radiation)

Reflection			θ_{obs} (°)	θ_{calc} (°)	d_{calc} (Å)	I_{calc}		I_{obs}
h	k	l				β-structure	ϵ-structure	
0	0	2	5.55	5.57	7.946	10.3	22.6	mw
0	0	4	11.15	11.19	3.973	34.1	68.9	vs
1	0	0	14.03	13.84	3.222	73.0	24.5	ms
1	0	1		14.13	3.157	14.9	88.1	
1	0	2	–	14.96	2.986	1.6	25.3	abs
1	0	3	16.29	16.26	2.753	100.0	100.0	ms
0	0	6	–	16.92	2.649	0.0	0.6	abs
1	0	4	18.01	17.94	2.502	14.8	11.6	vw
1	0	5	19.94	19.92	2.263	32.6	28.6	vw–w
1	0	6	–	22.13	2.046	0.0	31.3	abs
0	0	8	22.85	22.83	1.986	6.0	2.3	vvw
1	1	0	24.56	24.49	1.860	59.0	79.3	vvs
1	0	7		24.54	1.856	70.6	83.3	
1	1	2	25.20	25.19	1.811	1.6	3.3	vvw
1	0	8	27.26	27.12	1.691	5.4	7.5	s
1	1	4		27.23	1.685	17.3	35.0	
2	0	0	28.74	28.59	1.611	9.2	3.1	w
2	0	1		28.75	1.603	2.1	11.6	
0	0	10	29.03	29.02	1.589	3.2	3.7	vw–w
2	0	2		29.23	1.579	0.2	3.7	
1	0	9	30.02	29.86	1.548	0.7	4.5	vw–w
2	0	3		30.01	1.541	16.5	16.5	
1	1	6	–	30.43	1.522	0.0	0.7	abs
2	0	4	31.11	31.09	1.493	2.9	2.3	vvw
2	0	5	32.61	32.45	1.437	7.5	6.6	vvw
1	0	10		32.74	1.425	3.3	3.9	
2	0	6	34.05	34.06	1.376	0.0	8.4	vvw
1	1	8	34.62	34.60	1.358	10.1	3.8	vvw
0	0	12	35.65	35.60	1.324	3.2	2.7	mw
1	0	11	35.87	35.79	1.318	0.8	7.6	mw
2	0	7		35.93	1.314	22.0	26.1	
2	0	8	–	38.03	1.251	1.9	2.7	abs

TABLE IV A comparison of the experimentally-observed and computed X-ray powder intensity data for the β- and ϵ-type structures of $GaS_{0.25}Se_{0.75}$ (CuKα radiation)

Reflection			θ_{obs} (°)	θ_{calc} (°)	d_{calc} (Å)	I_{calc}		I_{obs}
h	k	l				β-structure	ϵ-structure	
0	0	2	5.57	5.59	7.917	12.4	25.5	mw
0	0	4	11.16	11.23	3.958	36.7	69.9	vs
1	0	0	13.87	13.88	3.213	76.2	25.3	vs
1	0	1	14.17	14.17	3.149	17.2	93.0	w–mw
1	0	2	14.99	15.01	2.977	2.0	26.4	vvw
1	0	3	16.26	16.31	2.744	100.0	100.0	vs
0	0	6	–	16.99	2.639	0.0	0.9	abs
1	0	4	17.94	18.00	2.495	15.9	11.5	m
1	0	5	19.93	19.99	2.255	34.2	30.3	m
1	0	6	–	22.21	2.039	0.0	32.3	abs
0	0	8	22.94	22.92	1.979	6.0	2.5	vvw
1	1	0	24.57	24.56	1.855	61.4	81.4	vvs
1	0	7		24.63	1.850	74.5	85.5	
1	1	2	25.25	25.27	1.806	1.9	3.8	vvw
1	0	8	27.27	27.22	1.685	5.3	7.8	ms
1	1	4		27.32	1.680	18.5	35.3	
2	0	0	28.68	28.68	1.606	9.6	3.2	mw–m
2	0	1		28.84	1.598	2.4	12.3	
0	0	10	–	29.14	1.583	3.1	3.7	abs
2	0	2	–	29.32	1.574	0.3	3.8	abs
1	0	9	30.09	29.97	1.543	0.7	4.5	m–ms
2	0	3		30.11	1.537	16.5	16.4	
1	1	6	–	30.53	1.518	0.1	1.0	abs
2	0	4	31.19	31.19	1.489	3.1	2.2	vw–w
2	0	5	32.51	32.55	1.433	7.8	7.0	vw–w
1	0	10		32.87	1.420	3.2	3.8	
2	0	6	–	34.18	1.372	0.0	8.7	abs
1	1	8	34.68	34.72	1.353	10.0	4.1	vvw
0	0	12	35.91	35.75	1.319	3.4	2.8	m
1	0	11		35.93	1.314	1.2	7.7	
2	0	7		36.06	1.310	23.3	26.7	
2	0	8	–	38.17	1.247	1.9	2.8	abs
1	0	12	39.15	39.17	1.221	4.0	1.3	vvw

compounds with compositions in the range $0.25 \leqslant x \leqslant 1.0$ fitted well with structure factors and intensities derived from the β-structure of Hahn and Franck [17]. The β-structure is, in any case, expected to be here more stable energetically than the ϵ-structure [20]. Laue photographs of GaS crystals indicated that they were unstrained in the "as-grown" condition, but that strain increased rapidly with slight mechanical handling.

Comparison of X-ray intensities for the β- and ϵ-structures with those from GaSe showed that it was very difficult to distinguish between the two structures from powder photographs alone. All single crystal studies of the GaSe structure describe only the ϵ, γ, or δ forms [4]. Because the atomic scattering factors of Ga and Se are alike the most noticeable difference between the intensities of the β and ϵ forms (see, for example, Tables III and IV) lies in the relative magnitudes of the reflections $(1\,0\,\bar{1}\,0)$ and $(1\,0\,\bar{1}\,1)$. However, these lines overlap on the powder photographs of GaSe because of the line broadening referred to above, and do not therefore differentiate between the structures. Among the weaker reflections the absence of the $(1\,0\,\bar{1}\,2)$ and the $(1\,0\,\bar{1}\,6)$ from the observed reflections suggests the β-structure. These reflections are, however, greatly weakened by the process of powdering [5].

At intermediate compositions, between $0.25 \leqslant x \leqslant 1.0$, clear resolution of the $(1\,0\,\bar{1}\,0)$ and $(1\,0\,\bar{1}\,1)$ reflections allowed the β-structure to be positively identified. At values of x between 0 and 0.25, line broadening again caused overlap of these and other reflections, and prevented clear identification.

Although the presence and magnitude of the

c-parameter discontinuity is therefore not fully explained, it is thought to correspond to the structural transformation from the β-form of GaS to the ϵ-form of GaSe. The variation of lattice parameter suggests that this is an abrupt transition at $x = 0.25$. However, examination of structure factors suggests that the transition is not a sudden one, and this is supported by the study of surface growth features. Formation of either of the two alternative structures may occur over the composition range $0.2 \leqslant x \leqslant 0.3$.

3. Non-stoichiometric phases

The crystallography of non-stoichiometric phases Ga_ySe in the Ga–Se system is described by Terhell and Lieth [5], who showed that a continuous range of non-stoichiometric compounds could be obtained by varying the composition of the initial mix of elements in the growth ampoule. Similar experiments performed as part of the present investigation showed that the composition of the initial ampoule charge could be reduced to GA : Se = 0.75 : 1 before traces of the cubic material Ga_2Se_3 started to form.

Since no earlier results are available concerning the non-stoichiometric phases Ga_yS in the system Ga–S, attempts were made to grow such non-stoichiometric materials by varying the charge composition away from GaS within the range $0.5 \leqslant y \leqslant 1.5$. The growth conditions used were the optimum ones determined for the transport of GaS [13].

For all values of y between 1.0 and 1.5, yellow plate-like single crystals were transported which were virtually indistinguishable from GaS both visually and by X-ray diffraction. Measurement of composition by the oxide reduction technique, however, indicated compositions between $Ga_{1.03 \pm 0.03}S$ and $Ga_{1.11 \pm 0.03}S$, depending on the amount of excess gallium in the charge. The unused gallium remained in elementary form in the untransported residue at the reaction end of the ampoule.

When y decreased from 1.0 towards 0.5, a two-phase mixture emerged at $y = 0.8$. One phase consisted of yellow plates indistinguishable by X-ray methods from GaS. The second phase took the form of small (1 to 2 mm) ivory coloured crystals. No intergrowth of the two phases obtained and a clear line of demarcation existed between them in the ampoule. Between $0.7 \geqslant y \geqslant 0.5$ only the ivory coloured crystals were transported. This second phase has a composition $Ga_{0.68 \pm 0.03}S$ and was identified from X-ray powder photographs as α-Ga_2S_3 [21]; the suggestion [22] that it might be a sulphur-rich form of Ga_2S_3 is thought to be incorrect. The dark-red form of Ga_2S_3 described by Lieth *et al.* [22] was not observed in the present study.

Acknowledgements

The authors wish to thank Dr N. Pentland, OBE, Head of the Department of Applied Physics at Brighton Polytechnic, for research facilities, and Dr E.A. Kellett, now at the Hosiery and Allied Trades Research Association, Nottingham, for his valued discussions and advice.

References

1. H. HAHN, *Angew. Chem.* **65** (1953) 538.
2. F. JELLINEK and H. HAHN, *Z. Naturforsch* **16** (1961) 713.
3. K. SCHUBERT, E. DÖRRE and H. KLUGE, *Z. Metallkunde* **46** (1955) 216.
4. A. KUHN, R. CHEVALIER and A. RIMSKI, *Acta Cryst.* **B31** (1975) 2841.
5. J.C.J.M. TERHELL and R.M.A. LIETH, *Phys. Stat. Sol. (a)* **10** (1972) 529.
6. C. MANFREDOTTI, A. RIZZO, A. BUFO and V.L. CARDETTA, *ibid.* **30** (1975) 375.
7. G. ARANCIA, M. GRANDOLFO, C. MANFREDOTTI and A. RIZZO, *ibid.* **33** (1976) 563.
8. J.C.J.M. TERHELL and R.M.A. LIETH, *ibid.* **5** (1971) 719.
9. R.H. BUBE and E.L. LIND, *Phys. Rev.* **119** (1960) 1353.
10. J.L. BREBNER, *J. Phys. Chem. Solids* **25** (1969) 1927.
11. H.U. BOLSTERLI and E. MOOSER, *Helv. Phys. Acta.* **35** (1962) 538.
12. N. ROMEO, *J. Appl. Phys.* **42** (1971) 3643.
13. C.R. WHITEHOUSE and A.A. BALCHIN, *J. Crystal Growth* **43** (1978) 727.
14. R.H. WILLIAMS, *Trans. Faraday Soc.* **66** (1970) 1113.
15. A. KUHN, A. CHEVY and E. LENDVAY, *J. Crystal Growth* **13/14** (1972) 380.
16. E. LENDVAY, A. KUHN, A. CHEVY and T. CEVA, *J. Mater. Sci.* **6** (1971) 305.
17. H. HAHN and G. FRANCK, *Z. Anorg. Allg. Chem.* **278** (1955) 340.
18. K. SCHUBERT and E. DÖRRE, *Naturwissenschaften* **40** (1953) 604.
19. H. SUZUKI and R. MORI, *Japan. J. Appl. Phys.* **13** (1974) 417.
20. Z.S. BASINSKI, D.B. DORE and E. MOOSER, *Helv. Phys. Acta.* **34** (1961) 393.
21. J. GOODYEAR and G.A. STEIGMANN, *Acta Cryst.* **16** (1963) 946.
22. R.M.A. LIETH, H.J.M. HEIJHGERS and C.W.M. van der HEIJDEN, *J. Electrochem. Soc.* **113** (1966) 798.

Received 20 January and accepted 18 April 1978.